International Journal of Medical Microbiology 303 (2013) 190–200

Contents lists available at SciVerse ScienceDirect

International Journal of Medical Microbiology

journal homepage: www.elsevier.com/locate/ijmm

Methylthioadenosine/S-adenosylhomocysteine nucleosidase (Pfs) of *Staphylococcus aureus* is essential for the virulence independent of LuxS/AI-2 system

Yan Bao, Yajuan Li, Qiu Jiang, Liping Zhao, Ting Xue, Bing Hu*, Baolin Sun**

Hefei National Laboratory for Physical Sciences at the Microscale and School of Life Sciences, University of Science and Technology of China, Hefei, Anhui 230027, China

ARTICLE INFO

Article history:
Received 16 October 2012
Received in revised form 22 January 2013
Accepted 24 March 2013

Keywords:
Staphylococcus aureus
pfs
Extracellular protease
Virulence
Mouse
Zebrafish

ABSTRACT

Staphylococcus aureus is a major cause of infectious morbidity and mortality in both community and hospital settings. The bacterium continues to cause diverse invasive, life-threatening infections, such as pneumonia, endocarditis, and septicemia. Methylthioadenosine/S-adenosylhomocysteine nucleosidase (Pfs) is predicted to be an important enzyme involved in methylation reactions, polyamine synthesis, vitamin synthesis, and quorum sensing pathways. For the first time, we demonstrate that Pfs is essential for the virulence of *S. aureus*. The *pfs* mutant strain, as compared to the isogenic wild type, displayed a decreased production of extracellular proteases, which was correlated with a dramatic decrease in the expression of the *sspABC* operon and a moderate decrease of *aur* expression. The mouse model of sepsis and subcutaneous abscesses indicated that the *pfs* mutant strain displayed highly impaired virulence compared to the isogenic wild type. The decreased virulence of the *pfs* mutant strain is in correspondence with its decreased proliferation in vivo, indicated with a real-time analysis in the transparent system of zebrafish embryos. These phenotypes of the *pfs* mutant strain are LuxS/AI-2 independent despite the essential role *pfs* plays in AI-2 production. Our data suggest that Pfs is a potential novel target for anti-infection therapy.

Introduction

Staphylococcus aureus can induce diverse invasive, life-threatening infections, such as pneumonia, endocarditis and septicaemia (Bubeck Wardenburg et al., 2007; Panizzi et al., 2011), and is a major cause of infectious morbidity and mortality in both community and hospital settings (Boucher and Corey, 2008; David and Daum, 2010). The worldwide emergence of antibiotic resistant strains continues unabated, along with an overall increase in the number of infections worldwide (Fridkin et al., 2005; Jain et al., 2011), highlighting the urgent need for new agents for the treatment of *S. aureus* infection. Non-conventional anti-infective approaches have been explored that are non-lethal to bacteria, where the potential to develop resistance is assumed to be less significant (Maresso and Schneewind, 2008; Wyatt et al., 2010).

As an activated group donor, S-adenosylmethionine (SAM) is essential in a broad array of metabolic reactions, such as methylation reactions, polyamine synthesis, SAM radical-mediated vitamin synthesis, and N-acyl-homoserine lactone (autoinducer-1) synthesis (Parveen and Cornell, 2011) (Fig. 1). Methylthioadenosine (MTA) (Pajula and Raina, 1979), S-adenosylhomocysteine (SAH) (Simms and Subbaramaiah, 1991), and 5′-deoxyadenosine (5′dADO) (Choi-Rhee and Cronan, 2005) are product inhibitors of these reactions, and MTA/SAH nucleosidase (Pfs) is the enzyme that catalyses their irreversible hydrolytic deadenylation reaction in bacteria (Della Ragione et al., 1985). Methylthioadenosine/S-adenosylhomocysteine nucleosidase is widespread among bacteria (Winzer et al., 2002). Sun and co-workers showed that 51 out of 138 bacterial species with completely sequenced genomes possess cytoplasmic MTA/SAH nucleosidase (Sun et al., 2004). It was reported that the inhibition of MTA/SAH nucleosidase activity led to an accumulation of MTA and SAH within bacterial cells (Heurlier et al., 2009) and ended into the inhibition of SAM-dependent synthase activities. In addition, Pfs is involved in the recycling pathway of adenine, sulphur, and methionine, and it also produces the universal quorum-sensing signal, autoinducer-2 (AI-2) (Heurlier et al., 2009).

On the basis of its importance in a wide array of metabolic reactions and as an enzyme present in most bacterial species but absent in humans, Pfs is an attractive target for developing new classes of broad-spectrum inhibitors for the treatment of bacterial infections (Parveen and Cornell, 2011). An evaluation of the substrate analogs and transition state analogs effective against MTA/SAH

* Corresponding author. Tel.: +86 551 6360 2489; fax: +86 551 6360 7014.
** Corresponding author. Tel.: +86 551 6360 6748; fax: +86 551 6360 7438.
E-mail addresses: bhu@ustc.edu.cn (B. Hu), sunb@ustc.edu.cn (B. Sun).

1438-4221/$ – see front matter © 2013 Elsevier GmbH. All rights reserved.
http://dx.doi.org/10.1016/j.ijmm.2013.03.004

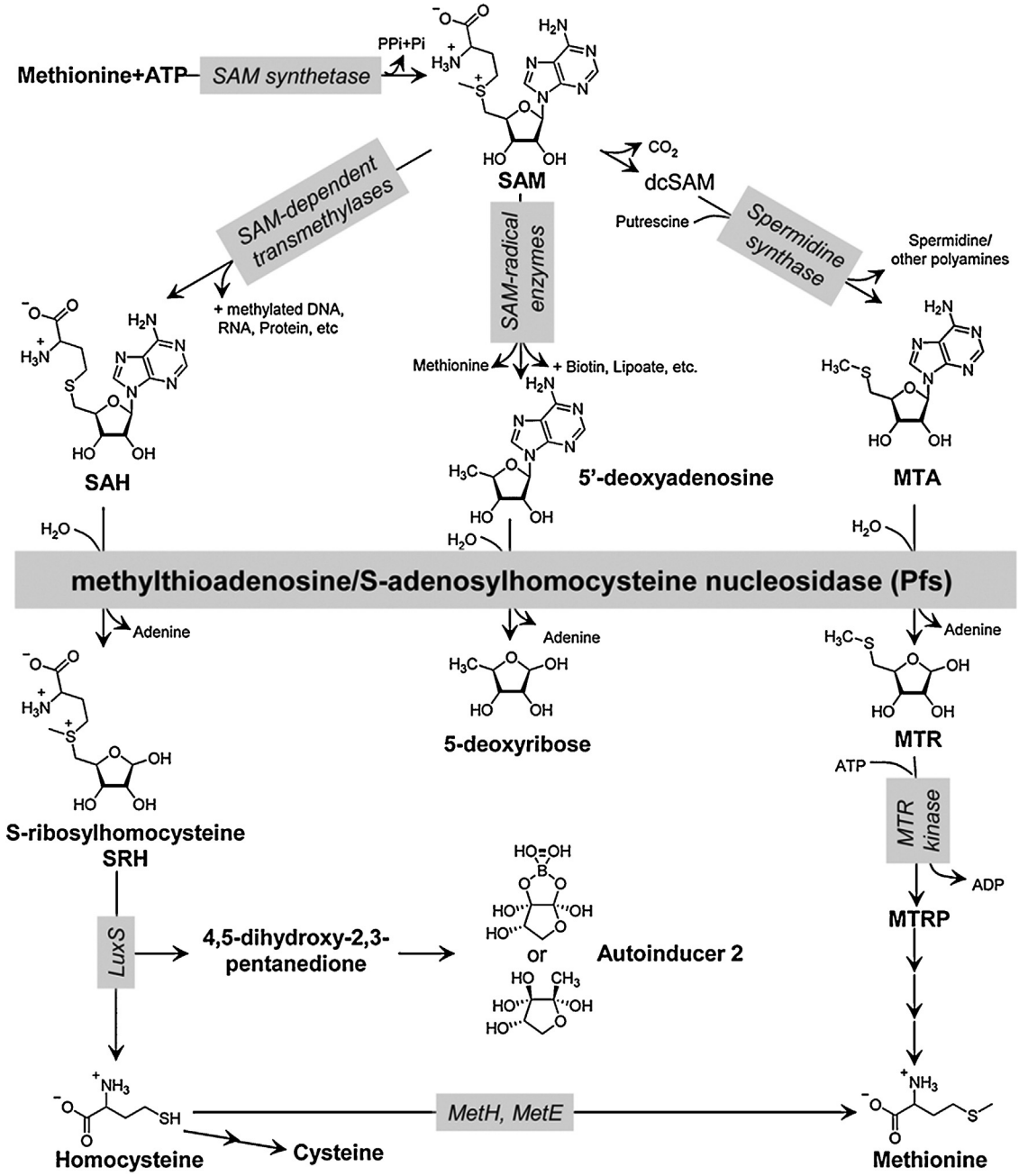

Fig. 1. Methylthioadenosine/S-adenosylhomocysteine nucleosidase (Pfs) is an integral component of the S-adenosylmethionine (SAM) pathway. As an activated group donor, SAM is essential in a broad array of metabolic reactions, such as methylation reactions, polyamine synthesis, and SAM radical-mediated vitamin synthesis (Parveen and Cornell, 2011). Methylthioadenosine (MTA) (Pajula and Raina, 1979), S-adenosylhomocysteine (SAH) (Simms and Subbaramaiah, 1991), and 5′-deoxyadenosine (5′dADO) (Choi-Rhee and Cronan, 2005) are product inhibitors of these reactions, and Pfs is the enzyme that catalyses their irreversible hydrolytic deadenylation reaction in bacteria (Della Ragione et al., 1985). It was reported that the inhibition of MTA/SAH nucleosidase activity led to an accumulation of MTA and SAH within bacterial cells (Heurlier et al., 2009) and ended into the inhibition of SAM-dependent synthase activities. In addition, Pfs is involved in the recycling pathway of adenine, sulphur, and methionine, and it also produces the universal quorum-sensing signal, autoinducer-2 (AI-2) (Heurlier et al., 2009).

nucleosidases of *Borrelia burgdorferi*, which uniquely expresses three homologous functional enzymes (Fraser et al., 1997; Parveen et al., 2006; Parveen and Leong, 2000), led to the identification of compounds that either inhibited the growth of these spirochaetes or showed bactericidal activities (Cornell et al., 2009). Using transition state analogs, the role of Pfs inhibitors has been explored in pathogenic strains of *Vibrio cholera* and *Escherichia coli*, where they can inhibit AI-2 production and reduce biofilm formation, but with minimal effect on bacterial growth (Gutierrez et al., 2009). These results indicate that the inhibition of this enzyme can affect the physiological activities of different bacteria. New inhibitors against Pfs are currently being explored for the development of potential novel broad-spectrum antimicrobials. However, despite this, the importance of Pfs independent of AI-2 remains generally underappreciated. Up to now, nothing is known about the role Pfs plays in the virulence of bacteria.

In *S. aureus*, the structure of Pfs was determined in a complex with the transition-state analog formycin A at a 1.7 Å resolution (Siu et al., 2008). It was highly conserved in the active-site residues and revealed an identical mode of inhibitor binding with available *E. coli* Pfs structures (Siu et al., 2008). Furthermore, it was confirmed that Pfs of *S. aureus* displays MTA and

Table 1
Bacterial strains and plasmids used in this study.

Strains and plasmids	Relevant genotype	Reference or source
Strains		
S. aureus		
WT	NCTC8325 Wild type	NARSA
RN4220	8325-4, r $^-$	NARSA
SBY1	8325 *pfs*::*ermB*	This study
SBY2	8325 pLI50	This study
SBY3	8325 *pfs*::*ermB* pLI50	This study
SBY4	8325 *pfs*::*ermB* pLIpfs	This study
SBY5	8325 pgfp	This study
SBY6	8325 *pfs*::*ermB* pgfp	This study
SX1	8325 *luxS*::*ermB*	Zhao (Zhao et al., 2010)
E. coli DH5α	Clone host strain	Laboratory stock
Plasmids pEASY-TB	Clone vector, Kan^r, Ap^r	Transgen
pEC1	pUC18 derivative. Source of *ermB* gene. Ap^r	Brückner (Brückner, 1997)
pBT2	Shuttle vector, temperature sensitive, Ap^r, Cm^r	Brückner (Brückner, 1997)
pBTpfs	pBT2 containing 403-bp upstream and 506-bp downstream fragments of *pfs* and *ermB* gene, Ap^r, Cm^r, Em^r	This study
pLI50	Shuttle cloning vector, Ap^r, Cm^r	Addgene
pLIpfs	pLI50 with *pfs* and its promoter, Ap^r, Cm^r	This study
pgfp	*gfp* expression with the promoter of S10 ribosomal gene in pALC1484 plasmid (Xiong et al., 2002), Ap^r, Cm^r	This study

Table 2
Oligonucleotides used in this study.

Primers	Sequence (5′–3′)[a]
Up-sapfs-f-KpnI	GCG**GGTACC**CAGTTCGTTTAACTGGAACAACCAT
Up-sapfs-r-HindIII	GCG**AAGCTT**GCAGCTGTATCATCAAGTCAAAC
Down-sapfs-r-SalI	GCG**GTCGAC**GTTCATAATTGTTGCTGTAAACTCG
Down-sapfs-f-XbaI	GCG**TCTAGA**ATCACTACAACGACAAGTATCATGA
pfs knock complement F (kpnI)	GCG**GGTACC**AAACTTGCGAACTAAACCCA
pfs knock complement R (salI)	GCG**GTCGAC**GACTATTTTGATTATTTTCAGCCAT
pfs-realtime-S	GTAGTGATTACCCAAAGTG
pfs-realtime-A	AAATGCTGTTGCGTCTG
SspA RT-S	CAATGTGGGAAAGTAAAGG
SspA RT-A	ATCGTTGGCAAAATGGA
SspB RT-S	GGTTTCAATGCTTATTTTATCACTAGGCGC
SspB RT-A	CCAGCAAATTGTTGTTGTGCTAGATCT
Aur RT-S	TGGTCGCACATTCACAA
Aur RT-A	CGTAAAGCGTCTCCCTC
ScpA RT-S	CAAGCATTAACAGAGCAG
ScpA RT-A	CCCGTGGGTCATCAT
rt-16S-f	CGTGGAGGGTCATTGGA
rt-16S-r	CGTTTACGGCGTGGACTA
pS10-f-EcoRI	CTGA**GAATTC**CCGTTCTTATGACTA
pS10-r-SmaI	CTGA**CCCGGG**CTTATTCGTCTACA

[a] The sequences in bold refer to the restriction endonuclease recognition sites.

SAH nucleosidase activity (Siu et al., 2008). Besides this, the biological role of Pfs in the Staphylococcaceae family remains unknown.

AI-2, shared by both Gram-positive and Gram-negative bacteria, is generally considered to be a universal language for intraspecies and interspecies communication (Vendeville et al., 2005). *S. aureus* possesses a functional *luxS* gene, which has been proved to be essential for AI-2 production (Doherty et al., 2006; Winzer et al., 2002). In addition, *S. aureus* LuxS/AI-2 system has been reported to regulate a range of behaviors, such as virulence-associated traits (Zhao et al., 2010), biofilm formation (Yu et al., 2012), and susceptibility to cell wall synthesis inhibitor antibiotics (Xue et al., 2013).

In this study, we aim to prove that Pfs is essential for the virulence of *S. aureus*. A molecular genetics approach of targeted mutagenesis was used, and the *pfs* mutant strain was compared to the isogenic wild type strain with respect to the pathogenesis-related traits. It was found that the *pfs* mutation decreased the extracellular proteases expression of *S. aureus*. And the animal models of mouse and zebrafish were used to confirm that Pfs contributes to the pathogenicity of *S. aureus*. In addition, our results show that despite the essential role *pfs* plays in AI-2 production, these phenotypes of the *pfs* mutant strain is LuxS/AI-2 independent.

Materials and methods

Bacterial strains and growth conditions

The phenotypic and genotypic properties of the bacterial strains and plasmids used in this study are listed in Table 1. The *S. aureus* strain RN4220, a restriction-deficient derivative of strain 8325-4, was used as the initial recipient for the transformation of plasmid constructs. All *E. coli* strains were grown in Luria Bertani (LB) medium (Oxoid), and all *S. aureus* strains were grown in tryptic soy broth (TSB) containing 0.25% glucose (Difco, Detroit, Mich.) at 37 °C with shaking, unless otherwise stated. When required, the media were supplemented with antibiotics at the following concentrations: 100 μg/ml of ampicillin, 15 μg/ml of chloramphenicol, and 2.5 μg/ml of erythromycin.

Construction of the isogenic NCTC8325 pfs deletion strain

A *pfs* mutant strain in the background of *S. aureus* NCTC8325 was generated according to Brückner et al. (Brückner, 1997). The coding sequence of the *pfs* gene was replaced with the coding sequence of the erythromycin resistance cassette (*ermB*) by a double crossover event. Briefly, a 506-bp fragment upstream (fragment 1) and a 403-bp fragment downstream (fragment 2) of *pfs* (SAOUHSC_01702) were amplified using genomic DNA of *S. aureus* NCTC8325 as the template, and erythromycin resistance gene *ermB* (fragment 3) was cut from plasmid pEC1 with the *Hin*dIII and *Xba*I restriction enzymes. The three fragments were ligated with fragment 3 inside and the ligation product was cloned into the temperature-sensitive shuttle vector pBT2. This deletion vector was constructed using *E. coli* DH5α. In *S. aureus* strain NCTC8325, gene inactivation was carried out as previously described by Brückner et al. (Brückner, 1997). The erythromycin-resistant and chloramphenicol-sensitive strains were screened. Verification that the *pfs* gene had been deleted was performed by polymerase chain reaction (PCR) amplification and finally by sequencing. The sequences of the oligonucleotides used in this study are listed in Table 2.

Complementation of the pfs deletion strain

Complementation of *pfs* mutation was achieved using a plasmid expressing the *pfs* gene under the control of its native promoter. A 1065-bp fragment encompassing the open reading frame of *pfs* and 338 bp upstream of the *pfs* translation start site were cloned into the shuttle plasmid pLI50. The recombinant plasmid from RN4220 was then electroporated into the *pfs* mutant in order to construct the complemented strain SBY4. As a control, the wild type NCTC8325 strain (WT) and the *pfs* mutant strain were also transformed with the empty plasmid pLI50, and resulted in the strains of SBY2 and SBY3, respectively.

RNA isolation

Overnight cultures were inoculated to an optical density of 0.01 at 600 nm into fresh TSB medium. Small-scale RNA was prepared from *S. aureus* cultures at variable growth phases (3–8.5 h). RNA isolation was performed as Wolz et al. described (Wolz et al., 2002). *S. aureus* cells were pelleted and lysed in 1 ml of RNAiso (TaKaRa) with 0.7 g of zirconia-silica beads (0.1 mm in diameter) in a high-speed homogenizer (IKA® T25 digital UlTRA-TURRAX®). Total RNA was isolated according to the standard protocol of RNAiso. The isolated RNA was treated with RNase-free DNase I (Takara) in order to remove the DNA template, and the concentration of RNA was quantified spectrophotometrically at 260 nm.

Quantitative real-time reverse transcription (RT)-PCR analysis

Real-time RT-PCR was carried out using the PrimeScript™ 1st strand cDNA Synthesis Kit and SYBR *Premix Ex Taq*™ (Takara) according to the manufacturer's instructions with the oligonucleotides shown in Table 2. Specific primers of each gene were used. Real-time PCR was performed using the StepOne™ Real-Time PCR System (Applied Biosystems). The housekeeping 16S rRNA gene was used as an endogenous control and the quantity of cDNA measured by real-time PCR was normalized to the abundance of 16S cDNA. The specificity of the PCR was confirmed by the melting curve of the products. In order to check for DNA contamination, each sample of RNA was subjected to PCR using SYBR *Premix Ex Taq*™ (Takara); no amplification products were detected.

Milk agar plates for detecting protease activity

Each milk agar plate consisted of 3 g/l TSB, 10 g/l non-fat dry milk, and 15 g/l agar. A volume of 2.5 μl of the cultures was spotted onto the milk agar plate and incubated at 37 °C for 3 days. The presence of transparent zones around the colonies was caused by protease activity.

Zymography of extracellular proteases

Zymography was conducted as described by Beenken et al. (2010). Supernatants were harvested from overnight (15 h) cultures, normalized based on the cell density of each culture prior to filter sterilization, and then concentrated 15-fold using Centricon YM-3 filter units (Millipore, Bedford, MA). For zymography, equivalent samples in a buffer without reducing agent were subjected to SDS-PAGE using 12% SDS-polyacrylamide gels containing gelatin (1 mg/ml). Following electrophoresis, the SDS was soaked out from the gel (zymogram) by shaking gently for 60 min at room temperature (RT) in renaturing buffer (2.5% TritonX-100), and then incubated overnight at 37 °C in activation buffer (0.2 M Tris, 5 mM $CaCl_2$, pH 7.4). In order to visualize the protease bands, the gels were then stained with Coomassie blue dye at room temperature for 2 h before being destained overnight in distilled water to reveal zones of protease activity.

Ethics statement

The use and care of mice in the present study followed strictly the guidelines adopted by the Ministry of Health of the People's Republic of China in June 2004. The protocol was approved by the Institutional Animal Care and Use Committee of the University of Science and Technology of China (USTCACUC1101053). All efforts were made to minimize the mice number and suffering. Zebrafish used in this study were handled in accordance with IACUC-approved protocols following standard procedures (www.zfin.org).

Mouse infection model

Male BALB/c mice were purchased from Shanghai Experimental Center, Chinese Science Academy (Shanghai, China), and housed in isolated cages in an animal facility under specific pathogen-free conditions. Overnight cultures of *S. aureus* isolates in TSB were collected, washed twice and diluted in sterile PBS. Viable staphylococci were counted via their colony-forming units (CFU) on TSB agar plates in order to quantify the infectious dose.

For the model of sepsis, mice were intravenously administered with a bacterial suspension or PBS via the tail vein and monitored daily for weight and death. At the indicated time after infection, the mice were killed and their organs were removed. The organs were homogenized in water and dilutions were plated onto TSB agar plates in order to measure the CFU of surviving cells.

The subcutaneous abscess model was established following the method of Liu et al. (2005). Bacterial cultures in PBS were mixed with an equivalent volume of sterilized Cytodex beads (Sigma) suspended in PBS at a concentration of 20 mg/ml. The mice were injected subcutaneously in both flanks of the back with the indicated culture. Lesion size, as assessed by the maximal length × width of the developing ulcers, was measured daily. The animals were killed 7 days after the injections. The skin lesions were excised and homogenized in water. The CFU recovered from each individual lesion was determined by serial dilution and plated onto TSB agar plates.

Zebrafish embryo infection models of S. aureus

Adult wild-type AB zebrafish were reared and propagated in recirculation systems and the embryos were incubated in Hank's medium at 28.5 °C. The embryos were collected from a laboratory-breeding colony kept at 28.5 °C with a 10:14 h light/dark cycle according to the standard protocols. The embryos were staged according to hours post fertilization (hpf) and morphological criteria. Embryos (30 hpf) were dechorionated by Pronase E (Roche) and sorted in fish water containing 0.003% phenylthiourea in order to prevent melanization. Cultures of *S. aureus* at an OD_{600} of 0.5 were collected, washed twice, and suspended in PBS supplemented with phenol red (0.5%, Sigma). For the control, this suspension was boiled at 100 °C for the preparation of heat-killed *S. aureus*. For the injection of *S. aureus*, embryos at 30–32 hpf were anaesthetized in 0.02% buffered 3-aminobenzoic acid methyl ester (MS222, Sigma). The embryos were then individually injected using pulled glass microcapillary pipettes filled with a bacterial suspension of a known concentration. Microinjections of the bacterial suspension were directed into pericardial of the embryos. The microinjections were performed using the following equipment: a pneumatic micropump (PICOSPRITZER III), a micromanipulator (KANETEC, MB-K), and a stereoscopic dissecting microscope (SM20, TECH). After the injections the embryos were incubated in Hank's medium in a 60 mm dish. An equal volume of bacteria was ejected into 1 ml of PBS in duplicate before and after the injection of each culture, and the CFU in PBS was counted; the injection dose was quantified as the mean CFU. Following infection, the embryos were frequently observed and any dead embryos were removed with numbers recorded at each time point.

GFP expression in S. aureus

The plasmid pgfp was constructed with GFP expressed under the control of the S10 protein promoter. The promoter of the S10

ribosomal gene was amplified from genomic DNA of *S. aureus* NCTC8325 and ligated between the restriction enzyme sites *Eco*RI and *Sma*I of pALC1484 (Xiong et al., 2002) containing a promoterless red-shifted *gfp* (gfp_{uvr}) reporter gene. Plasmid pgfp was confirmed by sequencing and then transformed into the wild type and *pfs* mutant strain of *S. aureus* NCTC8325 in order to construct the SBY5 and SBY6 strains, respectively.

Microscopic observations of zebrafish embryos

The embryos were immersed in a 0.3% (w/v) low-melting point agarose solution of Hank's medium. Living embryos were anaesthetized with 0.02% Tricaine in Hank's medium. Fluorescence microscopy was performed using an OLYMPUS FV-1000 (BX61WI) confocal microscope with a 10× OLYMPUS UPLFL object (NA 0.3). The software programs IMARIS 7.0 (Bitplane, Switzerland), Image J (NIH) and Adobe Photoshop CS2 9.0 were used for image processing.

Fluorescent integrated density (FID) in the region of interest

Quantification of the fluorescent images taken from individual embryos infected by GFP-expressing *S. aureus* was performed using Image J software (NIH). In brief, the total fluorescent intensity in the region of interest of each image from the infected larva was accumulated.

Statistical analysis

Experiments were performed in multiple replicates. The results are expressed as mean ± s.e.m. We used Prism 4 software for statistical analyses (GraphPad Software Inc.). No matching Two-way ANOVA was used to determine the difference significance with respect to the body weight and lesion size of mice infected with different *S. aureus* strains. Two-tailed unpaired *t*-test was used to compute *P* values for comparison of bacterial burden in heart and lesion skin of mice infected with different *S. aureus* strains. A log-rank test was used to compute *P* values in order to compare the Kaplan–Meier survival curves of mice infected with different *S. aureus* strains. Differences with a *P* value less than or equal to 0.05 were considered statistically significant.

Results

The pfs gene expression is growth phase dependent

In *S. aureus* NCTC8325, *pfs* (SAOUHSC_01702) is present between two hypothetical proteins with unknown functions (http://www.ncbi.nlm.nih.gov/). Downstream of *pfs* are a GTP-binding proteins containing YqeH (SAOUHSC_01700), a shikimate 5-dehydrogenase (SAOUHSC_01699), a nicotinate (nicotinamide) nucleotide adenylyltransferase (SAOUHSC_01697), a DNA internalization-related competence protein (SAOUHSC 01691), and seven hypothetical proteins. Upstream of *pfs* are an enterotoxin family protein (SAOUHSC_01705), a LamB/YcsF family protein (SAOUHSC_01708), a putative acetyl-CoA carboxylase/biotin carboxylase (SAOUHSC_01709), a putative acetyl-CoA carboxylase/biotin carboxyl carrier protein (SAOUHSC_01710), and four hypothetical proteins. Most of the genes around *pfs* are functionally unknown, and no obvious link was found between the functions of these genes.

The transcription profile of *pfs* in *S. aureus* NCTC8325 was determined using real-time RT PCR. RNA from the wild type strain of *S. aureus* NCTC8325 was isolated at different stages during growth in tryptic soy broth (TSB) medium and then subjected to real time RT-PCR with 16S rRNA as an endogenous control. It was found that the expression of *pfs* was subject to growth phase-dependent regulation, and the transcription level was higher at the logarithmic (log) phase and decreased in the stationary phase (Fig. 2).

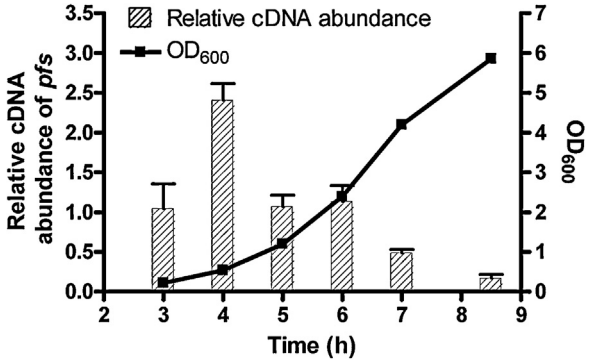

Fig. 2. Pfs expression is growth phase dependent. The profile of *pfs* transcription was determined by real-time PCR using cDNA prepared from mRNA samples obtained at different growth phases of *S. aureus* wild-type strain cultures in TSB medium, with 16S rRNA as an endogenous control. Data represents three independent analyses; error bars indicate SEM of three replicates.

Pfs is not essential for growth under nutrient-rich conditions, but is essential for AI-2 production in S. aureus

In order to determine the function of *pfs*, a *pfs* mutant strain (SBY1) was constructed in the background of *S. aureus* NCTC8325. In the complemented strain (SBY4), the *pfs* mutant strain was complemented by a wild-type allele of *pfs* on a plasmid under the control of its own promoter. As a control, strains of wild type (WT) and SBY1 were also transformed with the empty plasmid pLI50, named as SBY2 and SBY3, respectively (Table 1). As the important role Pfs plays in metabolism, the effect of *pfs* mutation on the growth of *S. aureus* was determined. The size of the colonies formed by the *pfs* mutant strain was almost the same as that of the wild type on the TSB agar plates. No significant difference was found in the growth of SBY3 compared with SBY2 or SBY4 in TSB liquid medium, and only a slightly delay was observed in the onset of the log phase of SBY3 for less than half an hour (Fig. S1A). The results indicated that the role of *pfs* in metabolism is unnecessary for the growth of *S. aureus* in TSB medium.

It has been reported that in several bacteria Pfs is essential for AI-2 production by providing substrate for AI-2 synthase-LuxS (Heurlier et al., 2009). To demonstrate this in the background of *S. aureus* NCTC8325, the presence of AI-2 in the culture supernatants was determined using the *V. harveyi* reporter strain BB170. Compared to SBY2, SBY3 completely lost the ability to produce AI-2, whereas AI-2 production was restored in SBY4 (Fig. 3), suggesting that the Pfs reaction is the sole intracellular source of AI-2 production.

The pfs mutation decreases the expression of extracellular proteases independent of AI-2 in S. aureus

In order to examine the contribution of Pfs to *S. aureus* pathogenesis, the SBY3 strain was compared with the SBY2 and SBY4 strains regarding pathogenesis-related traits. The *pfs* mutation had no obvious effect on haemolytic (Fig. S1B) or lipase activity (Fig. S1C), but decreased the activity of extracellular proteases (Fig. 4A). As shown in Fig. 4A, we can observe obvious zones of clearing around the colonies of SBY2 and SBY4, caused by protease activity. At the same time, the zone of clearing is visibly reduced around the colony of SBY3.

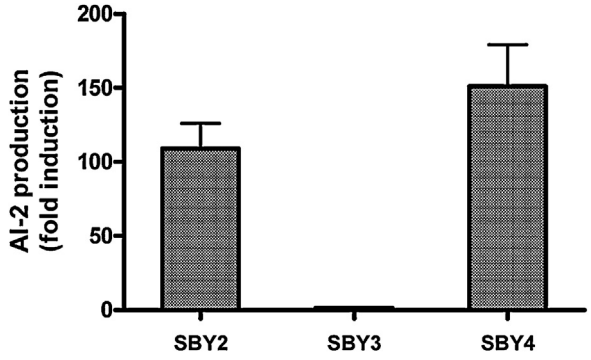

Fig. 3. Pfs is essential for AI-2 production in *S. aureus*. The production of AI-2 of the wild type strain (SBY2), the *pfs* mutant strain (SBY3), and the complemented strain (SBY4) was compared using the *V. harveyi* BB170 AI-2 reporter strain on cell-free supernatants of cultures. Data represents two independent analyses; error bars indicate SEM of three replicates.

As measured above, Pfs is essential for AI-2 production in *S. aureus*. AI-2 quorum sensing has been proved to be related to the regulation of protease expression (Brackman et al., 2011). Thus we wondered whether the protease expression deficiency of the *pfs* mutant strain is due to the defect of AI-2 production. We did not observe obvious difference of the extracellular protease level between the *luxS* mutant strain (SX1), which has been proved to be defect in AI-2 production (Zhao et al., 2010), and its isogenic wild type strain, displayed on the milk TSB agar plate (Fig. 4B). So thus we conclude that the decreased extracellular protease level of *pfs* mutant strain is LuxS/AI-2 independent.

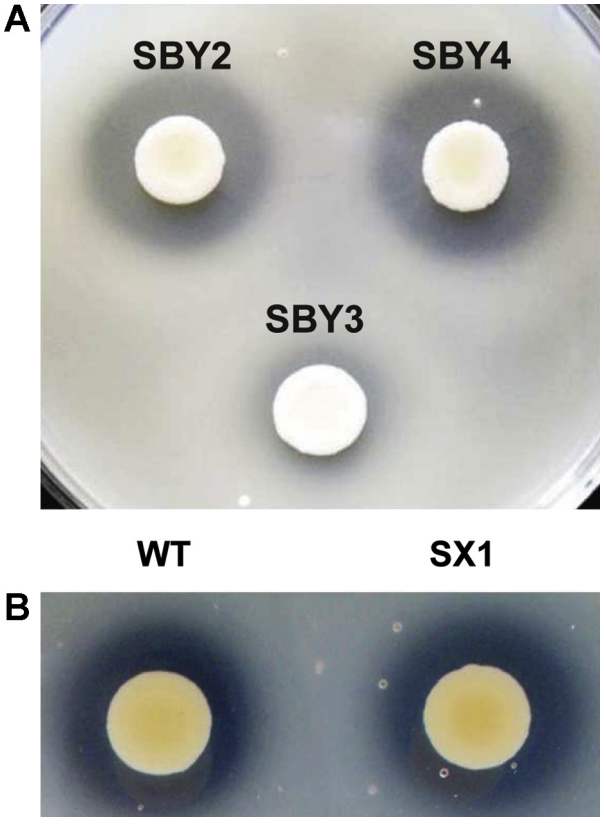

Fig. 4. The *pfs* mutation decreases the expression of extracellular proteases independent of LuxS/AI-2 system in *S. aureus*. (A) The *pfs* mutation decreases the extracellular protease activity on milk TSB agar plates. The image shows bacterial colonies of the wild type (SBY2), the *pfs* mutant (SBY3), and the complemented (SBY4) strains, and zones of clearing caused by protease activity. Data represents three independent analyses. (B) The comparison of the extracellular protease activity between the *luxS* mutant strain (SX1) and its isogenic wild type strain (NCTC8325, WT) on milk TSB agar plates. Data represents two independent analyses.

The decreased extracellular protease expression of the pfs mutant strain is related to the transcription reduction of sspABC operon and aur

Due to the decrease in extracellular protease activity of the *pfs* mutant strain in the milk plate, zymogram analyses were conducted to determine the differences in the profile of secreted proteases among the strains of SBY2, SBY3, and SBY4 by one-dimensional sodium dodecyl sulphate (SDS)-polyacrylamide gel electrophoresis. An obvious decrease in the proteolytic activity of two major extracellular proteases (SspA and SspB, as described by Shaw (Shaw et al., 2004)) was observed (Fig. 5A). The major proteolytic enzymes secreted by *S. aureus* were suggested to consist of a metalloproteinase (aureolysin, Aur), a serine glutamylendopeptidase (serine protease, SspA) and two related cysteine proteinases, referred to as staphopain (ScpA) and the cysteine protease (SspB) (Shaw et al., 2004). The transcription level of the four genes was compared through real-time RT PCR in strains of SBY2, SBY3, and SBY4. The transcription of *sspABC* operon and *aur* was induced at late phase of the growth (Fig. 5B-D), whereas that of *scpA* was higher at the early phase of the growth (Fig. S2). Consistent with the result of zymogram analyses, the *pfs* mutation resulted in a dramatic decrease in the transcription of the *sspABC* operon throughout the growth phase (Fig. 5B and C). And there is also a moderate decrease in *aur* transcription (Fig. 5D). The same transcriptional profile of *sspA* and *sspB* is in agreement with the previous identification of an operon structure encoding the secreted serine and cysteine proteases SspA and SspB of *S. aureus* (Rice et al., 2001). The transcription level of *scpA* was not affected by the knockout of *pfs* (Fig. S2). As the parental phenotype was restored in SBY4, we concluded that the differences between the *pfs* mutant and the wild type strain in extracellular protease expression were Pfs dependent and unlikely to be caused by second-site mutations or a polar effect on the downstream genes.

Pfs contributes to S. aureus sepsis infection of mice

Various roles in the infection process have been attributed to staphylococcal proteolytic enzymes (Dubin, 2002). Strains deficient in the *sspABC* operon showed reduced virulence in animal infection models (Coulter et al., 1998). Mouse infection models were used to investigate the significance of the extracellular protease expression defect to the virulence of the *pfs* mutant strain. The contribution of Pfs to invasive staphylococcal disease was determined in the mouse sepsis model, and BALB/c mice were infected by intravenous inoculations with *S. aureus* strains (Voyich et al., 2009).

At the challenge dose of 3×10^8 CFU, a 10-fold increase was observed in the survival rate of SBY3-infected mice compared to SBY2-infected ones ($P < 0.0001$), whereas the virulence was restored in the SBY4 strain (Fig. 6A). At the challenge dose of 1×10^8 CFU, the mortality of *S. aureus*-infected mice was low for both strains (Fig. S3A), and body weight change was set as the criteria for sickness determination. After infection with SBY3, the mice showed a rapid recovery in terms of body weight. The body weight of SBY3-infected mice was equal to that of the control mice 11 days post-infection (Fig. 6B). Infection with the wild type SBY2 clearly led to a more prominent loss of weight than the mutant. Although the gain of body weight of SBY2-infected mice was the same as for the control mice since 7 days after infection, the body weight of SBY2-infected mice was obviously lighter than the control ones as long as 49 days after infection (Fig. 6B). One day after infection with 3×10^8 CFU of *S. aureus*, the *S. aureus*-infected mice were killed and the organs were removed in order to determine the bacterial

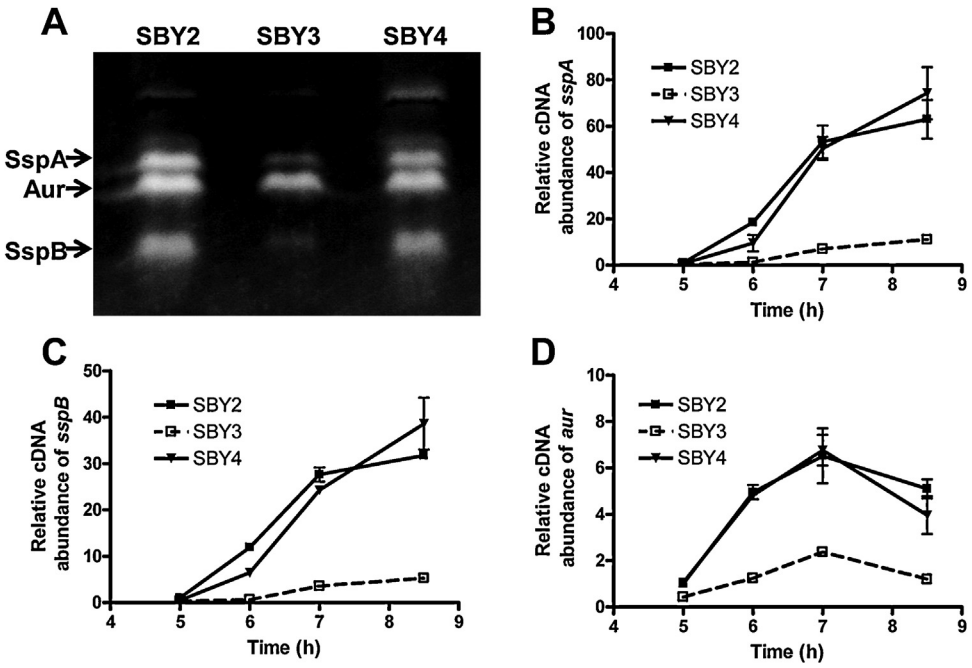

Fig. 5. The decreased extracellular protease expression of the *pfs* mutant strain is related to the transcription reduction of *sspABC* operon and *aur*. (A) Gelatin zymography. Protease activity of the overnight culture supernatants of the wild type (SBY2), the *pfs* mutant (SBY3), and the complemented (SBY4) strains was visualized using a zymogram gel containing gelatin as substrate. Protease activity appeared as a clear zone against a Coomassie blue-stained background. Data represents at least two independent analyses. Arrows indicate the activity of each protease, as determined previously (Shaw et al., 2004). (B–D) The *pfs* mutation reduced the transcription level of *sspA*, *sspB*, and *aur*. The transcriptional profile of *sspA* (B), *sspB* (C), and *aur* (D) of SBY3 was compared to that of SBY2 and SBY4 strains with the RNA isolated from the cultures of different growth phases (5–8.5 h). Data represents at least three independent analyses; error bars indicate SEM of three replicates.

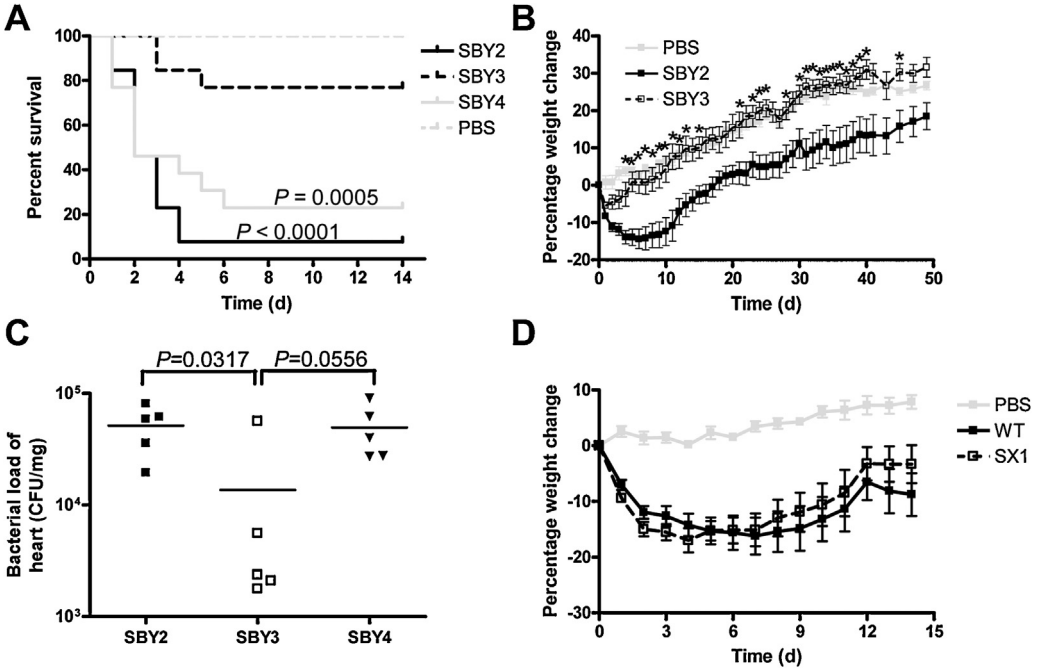

Fig. 6. Pfs contributes to the virulence of *S. aureus* in a mouse model of sepsis. (A) The survival rate of mice infected with the *pfs* mutant strain (SBY3) was greater than that of the wild type (SBY2) and the complemented (SBY4) strains. The Kaplan–Meier survival curves of mice infected via the tail vein with 3×10^8 CFU of SBY2, SBY3, and SBY4 ($n = 13$) was measured. The log-rank test was used to compute *P* values in order to compare SBY3 with SBY2 and SBY4. Data represents two independent analyses. (B) At the infection dose of 1×10^8 CFU, the body weight loss of SBY3-infected mice is decreased compared to that of SBY2 ($n = 10$). The mice injected with PBS were set as the normal control ($n = 4$). $^*P < 0.05$, SBY3 versus SBY2. Data represents two independent analyses. (C) The *pfs* mutation decreased the bacterial load in the heart of *S. aureus*-infected mice at the infection dose of 3×10^8 CFU. The staphylococcal burden in the heart of BALB/c mice ($n = 5$) infected with strains of SBY2, SBY3, or SBY4 was measured as CFU per milligram of tissue 1 day after infection. A two-tailed Student's *t*-test was used to compute *P* values in order to compare SBY3 with SBY2 and SBY4. (D) The mice were infected via the tail vein with 1×10^8 CFU of NCTC8325 (WT) or its isogenic *luxS* mutant strain (SX1) ($n = 12$). The body weight loss of *S. aureus*-infected mice was measured.

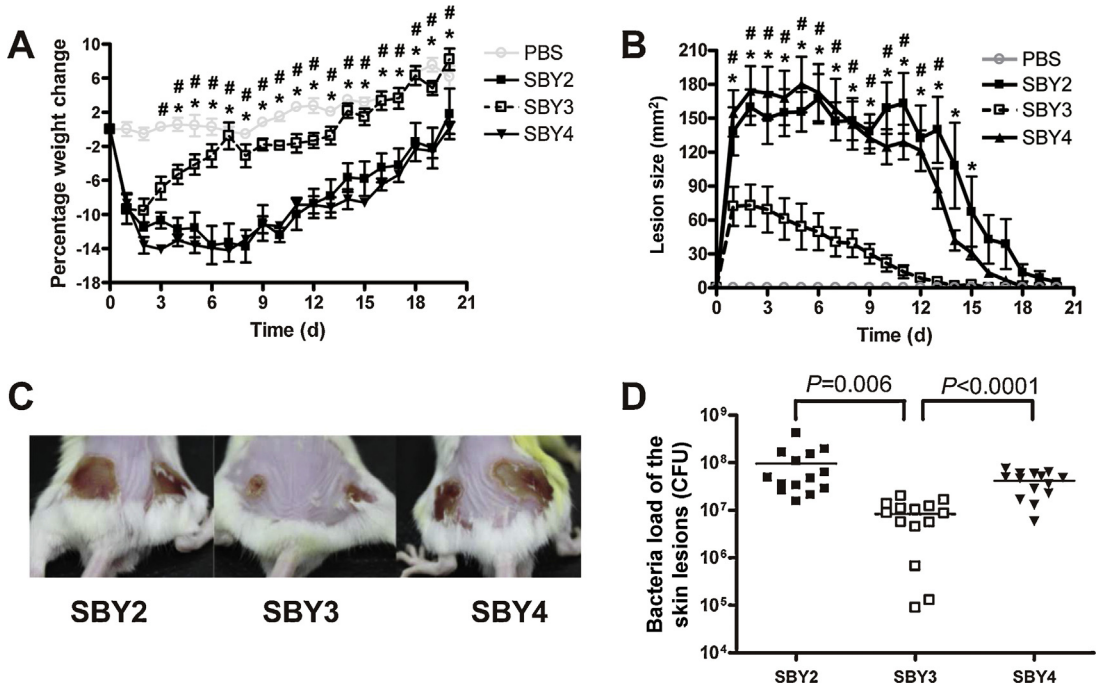

Fig. 7. Pfs contributes to virulence of *S. aureus* in a subcutaneous abscess model of mice. (A and B) Mice were subcutaneously injected in both flanks with cultures of the wild type (SBY2), the *pfs* mutant (SBY3), and the complemented (SBY4) strains at the injection dose of 7×10^7 CFU. The body weight of each individual mouse (A) ($n = 3$–5) and the size of each individual skin lesion (B) ($n = 6$–10) were monitored each day after infection. $^{*}P < 0.05$, SBY3 versus SBY2; $^{\#}P < 0.05$, SBY3 versus SBY4. Data represents three independent analyses. (C) The photographic images show a representative mouse from each treatment group 7 days after infection. (D) The lesions ($n = 14$) were harvested 7 days after infection and the CFU recovered from each individual lesion was determined. A two-tailed Student's *t*-test was used to compute *P* values in order to compare SBY3 with SBY2 and SBY4.

load (Gjertsson et al., 2012). A significant decrease in the bacterial load of the heart in SBY3-infected mice was detected compared to SBY2-infected mice, and the bacterial load was restored in the SBY4-infected mice (Fig. 6C).

To evaluate the contribution of LuxS/AI-2 system to the decreased virulence of the *pfs* mutant strain, the virulence of the *luxS* mutant strain was compared to the isogenic wild type strain in the mouse sepsis model. The mice were infected via the tail vein with 1×10^8 CFU of NCTC8325 (WT) or its isogenic *luxS* mutant strain (SX1) ($n = 12$). Through the measurement of the Kaplan–Meier survival curves (Fig. S3B) and the body weight loss (Fig. 6D) of *S. aureus*-infected mice, it was found that there was no statistic significant effect of *luxS* mutation on the virulence of *S. aureus*. So we conclude that the decreased virulence of the *pfs* mutant strain in the sepsis infection model of mice is LuxS/AI-2 independent.

Pfs is associated with S. aureus subcutaneous abscess infection of mice

The mouse subcutaneous abscess model was further used in order to assess the contribution of Pfs to the skin and soft tissue infection of *S. aureus* (Hruz et al., 2009). In these studies, mice were subcutaneously injected in both flanks with 7×10^7 CFU of *S. aureus* cultures for each site and the course of infection was monitored. Compared to SBY3-infected mice, the mice infected with SBY2 and SBY4 showed a greater degree of sickness, as indicated by a greater loss of body weight (Fig. 7A). As shown in Fig. 7B, the size of the skin lesions generated by SBY2 and SBY4 was significantly larger than those produced by SBY3, which was further demonstrated in photographs of the subcutaneous abscesses of *S. aureus*-infected mice 7 days post-infection (Fig. 7C). In parallel with its decreased lesion response, the SBY3-infected mice had a bacterial load in the lesion skin of about 1/10 of the SBY2-infected mice 7 days post-infection, and the bacterial load was restored in SBY4-infected mice (Fig. 7D).

The decreased virulence of the pfs mutant strain is in correspondence with its decreased proliferation in vivo

It has been measured that non-invasive, high-resolution, and long-term time-course experiments can be performed in the zebrafish embryos models to visualize infection dynamics with fluorescent markers (Tobin et al., 2012). The injection site chosen was the ventral aspect of the pericardium of the zebrafish embryos, 30 h post fertilization. Kaplan–Meier survival curves of zebrafish embryos ($n = 30$–40) infected at the pericardium site with 5000 CFU of SBY2, SBY3, and SBY4 were determined. The log-rank test was used to compute *P* values in order to compare SBY3 with SBY2 and SBY4. Significant attenuation of pathogenicity was observed for the *pfs* mutant strain compared to the wild type, and the virulence was restored in the complemented strain (Fig. 8A). The *S. aureus*-infected embryos were separated at the moment being found dead, homogenized, and the staphylococcal load was counted. The death of the *S. aureus*-infected embryos was associated with bacterial numbers in excess of 10^5 CFU per embryo, with few exceptions, and no difference was found between the strains (Fig. S4). It is thought that the decreased virulence of the *pfs* mutant strain is associated with a deficiency in the replication in embryos. GFP-expressing *S. aureus* strains (SBY5-the wild type *S. aureus* and SBY6-the *pfs* mutant strain) were used in order to monitor the infection process in real-time as previously described (Prajsnar et al., 2008). Time-lapse microscopy was performed and 3-D confocal images were taken for real-time analysis of in vivo staphylococcal proliferation within the embryos. Bacterial burdens were quantified in terms of fluorescent integrated density (FID) in images of the infected embryos (Adams et al., 2011). Increased survival was associated with a decreased rate of bacterial proliferation in embryos infected

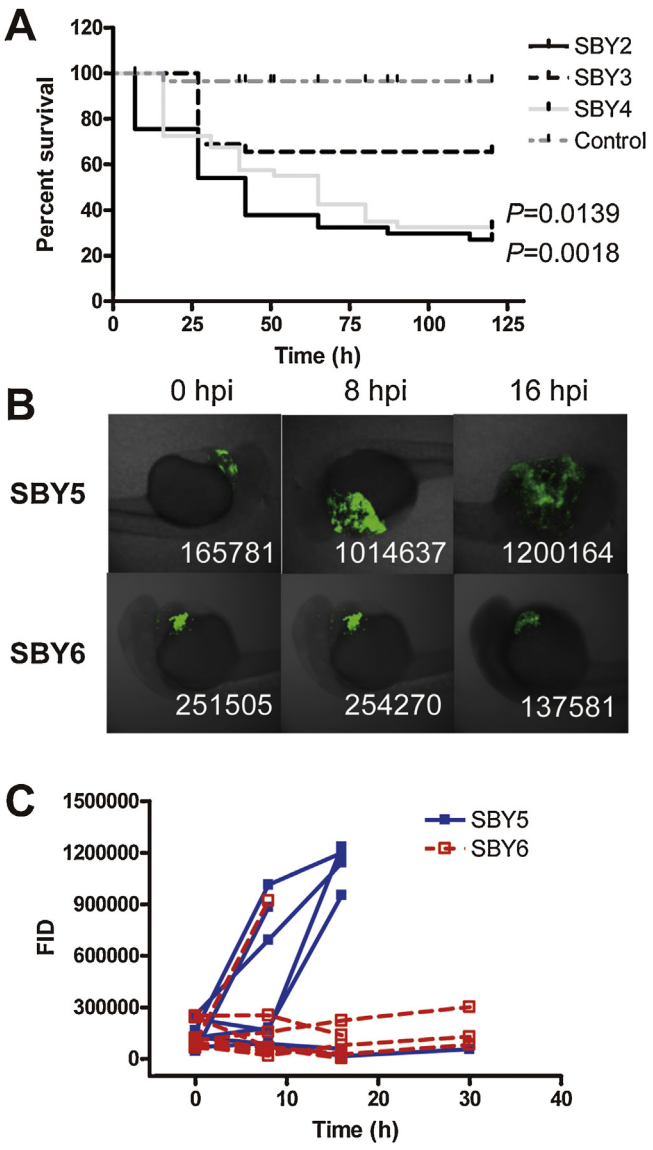

Fig. 8. The decreased virulence of the *pfs* mutant strain is in correspondence with its decreased proliferation in vivo. (A) The virulence of the *pfs* mutant strain (SBY3) was reduced in the pericardium infection model compared to the wild type (SBY2) and the complemented (SBY4) strains. Kaplan–Meier survival curves of zebrafish embryos ($n = 30–40$) infected at the pericardium site with 5000 CFU of SBY2, SBY3, and SBY4 were determined. The log-rank test was used to compute *P* values in order to compare SBY3 with SBY2 and SBY4. Data represents at least three independent analyses. (B) Proliferation in vivo was decreased in the *pfs* mutant strain in the pericardium infection model compared with the wild type. The GFP-expressing strains of the wild type (SBY5) and the *pfs* mutant (SBY6) were used. The real-time analysis of bacterial burdens was performed with confocal laser scanning microscopy. Fluorescence images of representative embryos infected with SBY5 or SBY6 are shown. The bacterial burdens were measured as fluorescent integrated density (FID) in images of infected embryos, and the FID values of each image are described in the picture. Data represents two independent analyses. Hpi represents hours post infection. (C) Quantity of FID analysis. FID values for individual embryos are plotted; data points from the same individual are connected. Data represents two independent analyses.

with the *pfs* mutant strain, as judged by fluorescence microscopy (Fig. 8B), and it was further confirmed quantitatively by FID analysis (Fig. 8C).

Discussion

Nowadays, the incessant emergence of antibiotic resistant strains has created new challenges in the treatment of bacterial infection. Despite its central role in cellular metabolism and quorum sensing, the importance of MTA/SAH nucleosidase (Pfs) in bacteria has only started to become appreciated in the past decade (Parveen and Cornell, 2011), and very little is known about the biological function of Pfs independent of the autoinducer AI-2. This study focused on revealing that Pfs plays an important role in the pathogenicity of *S. aureus*, and evaluating the possibility for Pfs as an anti-infection target.

For the first time, this study shows that Pfs is essential for the expression of extracellular proteases independent of LuxS/AI-2 system. Various roles in the infection process have been attributed to staphylococcal proteolytic enzymes (Dubin, 2002). Extracellular proteases are involved in the destruction of host tissues, which is a pronounced event in staphylococcal infections and allows the dissemination of bacteria and the acquisition of nutrients (Potempa et al., 1988; Travis et al., 1995). Also, dissemination in the host is further facilitated by the ability of extracellular protease to degrade the bacterial cell surface fibronectin-binding protein (FnBP) and, moreover, to affect the overall composition of surface proteins (McGavin et al., 1997). Extracellular proteases participate in the proteolytic processing of precursor forms including protease precursors, and they exert a pleiotropic effect on the profile of secreted proteins (Rice et al., 2001). In addition, the degradation of immunoglobulins and complement cascade proteins acts as a defence against the host immune response. In this study, the deletion of *pfs* decreased the activity of extracellular proteases of *S. aureus*, mainly because of the decreased expression of the *sspABC* operon. It was shown that strains deficient in the *sspABC* operon coding for serine (*sspA*) and cysteine (*sspB*) proteases showed highly reduced virulence in animal infection models, including abscess, systemic intravenous, and burn wound infection models of mouse (Coulter et al., 1998). The decreased extracellular protease level could be the reason for the decreased virulence of the *pfs* mutant strain.

Staphylococcus aureus is an adaptable, opportunistic pathogen that can infect a diverse range of tissues and cause a wide spectrum of diseases, and distinct molecular mechanisms are required for infection in different in vivo environments (Coulter et al., 1998). The systemic infection model measures the ability of the bacterium to adapt to the host environment, survive maximal exposure to host defence systems, and disseminate systemically (Coulter et al., 1998). The abscess model of focal infection, in contrast to the systemic infection model, does not require dissemination. During abscess formation, bacterial growth is curtailed by the influx of polymorphonuclear leukocytes, as well as oxygen and nutrient limitations (Coulter et al., 1998). The *pfs* mutation decreased the pathogenicity of *S. aureus* in both mice infection models. With a well-developed immune system (Trede et al., 2001; Zarkadis et al., 2001), which is quite similar to the mammalian immune system, the transparent system of zebrafish embryos was used for the real-time analysis of *S. aureus* infection. Consistent with the mouse models, the *pfs* mutant strain displayed decreased virulence, which corresponded to the decreased proliferation in vivo compared to the wild type. This means that the zebrafish embryo models, with its advantage of low cost, optical transparency during early development and easy large-scale breeding, could be chosen for the preliminary screening of drugs that target Pfs.

As the essential role Pfs plays in AI-2 production, we determined the dependence of the *pfs* mutant phenotypes on AI-2. As expected, Pfs is essential for AI-2 production in *S. aureus* NCTC8325, and possible effect of LuxS/AI-2 system on Pfs related phenotypes was investigated in this work. Doherty et al. showed that the inactivation of LuxS (AI-2 synthase) in various *S. aureus* strains did not affect virulence-associated traits, such as protease production and haemolysis (Doherty et al., 2006). Our group has concentrated on the study of LuxS in *S. aureus* NCTC8325. Compared to the isogenic wild type, no transcriptional changes in the genes related to

the extracellular proteases were found in genome-wide microarray data of the *luxS* mutant strain of *S. aureus* (Zhao et al., 2010). In this study, we did not observe obvious differences in the extracellular protease level and the virulence in the mouse sepsis model between the *luxS* mutant and the isogenic wild type strains. These data suggest that the decreased extracellular protease level and virulence of the *pfs* mutant strain observed in our work are LuxS/AI-2 independent.

The inhibition of MTA/SAH nucleosidase activity is predicted to cause an accumulation of MTA and SAH within bacterial cells and lead to the inhibition of SAM-dependent synthase activities (Heurlier et al., 2009). The lack of polyamine biosynthesis in *S. aureus* (Anzaldi and Skaar, 2011) excludes the possibility of the involvement of polyamine in these phenotypes. It was suspected that these phenotypes are due to methyl cycle or SAM-radical enzymes dependent processes. The metabolism processes Pfs participated are complicated and the relationships between Pfs and these phenotypes independent of LuxS/AI-2 system have not been reported. The effects of Pfs should be extensive and complex, and future research is necessary to gain mechanistic insights into how Pfs contributes to the regulation of extracellular protease expression and virulence. In this work, our concentration is to evaluate the possibility for Pfs as an anti-infection target.

Collectively, this study demonstrated that the *pfs* mutation in *S. aureus* NCTC8325 led to decreased virulence, which could turn Pfs into an anti-infection drug target. Given the conservation of Pfs in a wide variety of bacterial species, it is possible that the role of Pfs in virulence is widely conserved. This study should facilitate further investigations into the role that Pfs plays in diverse bacterial species.

Acknowledgments

We thank the Network on Antimicrobial Resistance in *Staphylococcus aureus* (NARSA) for providing the bacterial strains. This work was supported by the National Natural Science Foundation of China (grants 31070116 and 31021061).

Appendix A. Supplementary data

Supplementary data associated with this article can be found, in the online version, at http://dx.doi.org/10.1016/j.ijmm.2013.03.004.

References

Adams, K.N., Takaki, K., Connolly, L.E., Wiedenhoft, H., Winglee, K., Humbert, O., Edelstein, P.H., Cosma, C.L., Ramakrishnan, L., 2011. Drug tolerance in replicating mycobacteria mediated by a macrophage-induced efflux mechanism. Cell 145, 39–53.

Anzaldi, L.L., Skaar, E.P., 2011. The evolution of a superbug: how Staphylococcus aureus overcomes its unique susceptibility to polyamines. Mol. Microbiol. 82, 1–3.

Beenken, K.E., Mrak, L.N., Griffin, L.M., Zielinska, A.K., Shaw, L.N., Rice, K.C., Horswill, A.R., Bayles, K.W., Smeltzer, M.S., 2010. Epistatic relationships between sarA and agr in Staphylococcus aureus biofilm formation. PLoS One 5, e10790.

Boucher, H.W., Corey, G.R., 2008. Epidemiology of methicillin-resistant Staphylococcus aureus. Clin. Infect. Dis. 46 (Suppl. 5), S344–S349.

Brackman, G., Celen, S., Hillaert, U., Van Calenbergh, S., Cos, P., Maes, L., Nelis, H.J., Coenye, T., 2011. Structure–activity relationship of cinnamaldehyde analogs as inhibitors of AI-2 based quorum sensing and their effect on virulence of Vibrio spp. PLoS One 6, e16084.

Brückner, R., 1997. Gene replacement in Staphylococcus carnosus and Staphylococcus xylosus. FEMS Microbiol. Lett. 151, 1–8.

Bubeck Wardenburg, J., Bae, T., Otto, M., Deleo, F.R., Schneewind, O., 2007. Poring over pores: alpha-hemolysin and Panton-Valentine leukocidin in Staphylococcus aureus pneumonia. Nat. Med. 13, 1405–1406.

Choi-Rhee, E., Cronan, J.E., 2005. A nucleosidase required for in vivo function of the S-adenosyl-L-methionine radical enzyme, biotin synthase. Chem. Biol. 12, 589–593.

Cornell, K.A., Primus, S., Martinez, J.A., Parveen, N., 2009. Assessment of methylthioadenosine/S-adenosylhomocysteine nucleosidases of Borrelia burgdorferi as targets for novel antimicrobials using a novel high-throughput method. J. Antimicrob. Chemother. 63, 1163–1172.

Coulter, S.N., Schwan, W.R., Ng, E.Y.W., Langhorne, M.H., Ritchie, H.D., Westbrock-Wadman, S., Hufnagle, W.O., Folger, K.R., Bayer, A.S., Stover, C.K., 1998. Staphylococcus aureus genetic loci impacting growth and survival in multiple infection environments. Mol. Microbiol. 30, 393–404.

David, M.Z., Daum, R.S., 2010. Community-associated methicillin-resistant Staphylococcus aureus: epidemiology and clinical consequences of an emerging epidemic. Clin. Microbiol. Rev. 23, 616–687.

Della Ragione, F., Porcelli, M., Carteni-Farina, M., Zappia, V., Pegg, A.E., 1985. Escherichia coli S-adenosylhomocysteine/5′-methylthioadenosine nucleosidase. Purification, substrate specificity and mechanism of action. Biochem. J. 232, 335–341.

Doherty, N., Holden, M.T., Qazi, S.N., Williams, P., Winzer, K., 2006. Functional analysis of luxS in Staphylococcus aureus reveals a role in metabolism but not quorum sensing. J. Bacteriol. 188, 2885–2897.

Dubin, G., 2002. Extracellular proteases of Staphylococcus spp. Biol. Chem. 383, 1075–1086.

Fraser, C.M., Casjens, S., Huang, W.M., Sutton, G.G., Clayton, R., Lathigra, R., White, O., Ketchum, K.A., Dodson, R., Hickey, E.K., Gwinn, M., Dougherty, B., Tomb, J.F., Fleischmann, R.D., Richardson, D., Peterson, J., Kerlavage, A.R., Quackenbush, J., Salzberg, S., Hanson, M., van Vugt, R., Palmer, N., Adams, M.D., Gocayne, J., Weidman, J., Utterback, T., Watthey, L., McDonald, L., Artiach, P., Bowman, C., Garland, S., Fuji, C., Cotton, M.D., Horst, K., Roberts, K., Hatch, B., Smith, H.O., Venter, J.C., 1997. Genomic sequence of a Lyme disease spirochaete, Borrelia burgdorferi. Nature 390, 580–586.

Fridkin, S.K., Hageman, J.C., Morrison, M., Sanza, L.T., Como-Sabetti, K., Jernigan, J.A., Harriman, K., Harrison, L.H., Lynfield, R., Farley, M.M., 2005. Methicillin-resistant Staphylococcus aureus disease in three communities. N. Engl. J. Med. 352, 1436–1444.

Gjertsson, I., Jonsson, I.M., Peschel, A., Tarkowski, A., Lindholm, C., 2012. Formylated peptides are important virulence factors in Staphylococcus aureus arthritis in mice. J. Infect. Dis. 205, 305–311.

Gutierrez, J.A., Crowder, T., Rinaldo-Matthis, A., Ho, M.-C., Almo, S.C., Schramm, V.L., 2009. Transition state analogs of 5′-methylthioadenosine nucleosidase disrupt quorum sensing. Nat. Chem. Biol. 5, 251–257.

Heurlier, K., Vendeville, A., Halliday, N., Green, A., Winzer, K., Tang, C.M., Hardie, K.R., 2009. Growth deficiencies of Neisseria meningitidis pfs and luxS mutants are not due to inactivation of quorum sensing. J. Bacteriol. 191, 1293–1302.

Hruz, P., Zinkernagel, A.S., Jenikova, G., Botwin, G.J., Hugot, J.P., Karin, M., Nizet, V., Eckmann, L., 2009. NOD2 contributes to cutaneous defense against Staphylococcus aureus through {alpha}-toxin-dependent innate immune activation. Proc. Natl. Acad. Sci. U. S. A. 106, 12873–12878.

Jain, R., Kralovic, S.M., Evans, M.E., Ambrose, M., Simbartl, L.A., Obrosky, D.S., Render, M.L., Freyberg, R.W., Jernigan, J.A., Muder, R.R., Miller, L.J., Roselle, G.A., 2011. Veterans Affairs initiative to prevent methicillin-resistant Staphylococcus aureus infections. N. Engl. J. Med. 364, 1419–1430.

Liu, G.Y., Essex, A., Buchanan, J.T., Datta, V., Hoffman, H.M., Bastian, J.F., Fierer, J., Nizet, V., 2005. Staphylococcus aureus golden pigment impairs neutrophil killing and promotes virulence through its antioxidant activity. J. Exp. Med. 202, 209–215.

Maresso, A.W., Schneewind, O., 2008. Sortase as a target of anti-infective therapy. Pharmacol. Rev. 60, 128–141.

McGavin, M.J., Zahradka, C., Rice, K., Scott, J.E., 1997. Modification of the Staphylococcus aureus fibronectin binding phenotype by V8 protease. Infect. Immun. 65, 2621–2628.

Pajula, R.L., Raina, A., 1979. Methylthioadenosine, a potent inhibitor of spermine synthase from bovine brain. FEBS Lett. 99, 343–345.

Panizzi, P., Nahrendorf, M., Figueiredo, J.L., Panizzi, J., Marinelli, B., Iwamoto, Y., Keliher, E., Maddur, A.A., Waterman, P., Kroh, H.K., Leuschner, F., Aikawa, E., Swirski, F.K., Pittet, M.J., Hackeng, T.M., Fuentes-Prior, P., Schneewind, O., Bock, P.E., Weissleder, R., 2011. In vivo detection of Staphylococcus aureus endocarditis by targeting pathogen-specific prothrombin activation. Nat. Med. 17, 1142–1146.

Parveen, N., Cornell, K.A., 2011. Methylthioadenosine/S-adenosylhomocysteine nucleosidase, a critical enzyme for bacterial metabolism. Mol. Microbiol. 79, 7–20.

Parveen, N., Cornell, K.A., Bono, J.L., Chamberland, C., Rosa, P., Leong, J.M., 2006. Bgp, a secreted glycosaminoglycan-binding protein of Borrelia burgdorferi strain N40, displays nucleosidase activity and is not essential for infection of immunodeficient mice. Infect. Immun. 74, 3016–3020.

Parveen, N., Leong, J.M., 2000. Identification of a candidate glycosaminoglycan-binding adhesin of the Lyme disease spirochete Borrelia burgdorferi. Mol. Microbiol. 35, 1220–1234.

Potempa, J., Dubin, A., Korzus, G., Travis, J., 1988. Degradation of elastin by a cysteine proteinase from Staphylococcus aureus. J. Biol. Chem. 263, 2664–2667.

Prajsnar, T.K., Cunliffe, V.T., Foster, S.J., Renshaw, S.A., 2008. A novel vertebrate model of Staphylococcus aureus infection reveals phagocyte-dependent resistance of zebrafish to non-host specialized pathogens. Cell. Microbiol. 10, 2312–2325.

Rice, K., Peralta, R., Bast, D., de Azavedo, J., McGavin, M.J., 2001. Description of staphylococcus serine protease (ssp) operon in Staphylococcus aureus and nonpolar inactivation of sspA-encoded serine protease. Infect. Immun. 69, 159–169.

Shaw, L., Golonka, E., Potempa, J., Foster, S.J., 2004. The role and regulation of the extracellular proteases of Staphylococcus aureus. Microbiology 150, 217–228.

Simms, S.A., Subbaramaiah, K., 1991. The kinetic mechanism of S-adenosyl-L-methionine: glutamylmethyltransferase from Salmonella typhimurium. J. Biol. Chem. 266, 12741–12746.

Siu, K.K.W., Lee, J.E., Smith, G.D., Horvatin-Mrakovcic, C., Howell, P.L., 2008. Structure of Staphylococcus aureus 5′-methylthioadenosine/S-adenosylhomocysteine nucleosidase. Acta Crystallogr. F – Struct. Biol. Cryst. Commun. 64, 343–350.

Sun, J., Daniel, R., Wagner-Dobler, I., Zeng, A.P., 2004. Is autoinducer-2 a universal signal for interspecies communication: a comparative genomic and phylogenetic analysis of the synthesis and signal transduction pathways. BMC Evol. Biol. 4, 36.

Tobin, D.M., May, R.C., Wheeler, R.T., 2012. Zebrafish: a see-through host and a fluorescent toolbox to probe host-pathogen interaction. PLoS Pathog. 8, e1002349.

Travis, J., Potempa, J., Maeda, H., 1995. Are bacterial proteinases pathogenic factors? Trends Microbiol. 3, 405–407.

Trede, N.S., Zapata, A., Zon, L.I., 2001. Fishing for lymphoid genes. Trends Immunol. 22, 302–307.

Vendeville, A., Winzer, K., Heurlier, K., Tang, C.M., Hardie, K.R., 2005. Making 'sense' of metabolism: autoinducer-2, LuxS and pathogenic bacteria. Nat. Rev. Microbiol. 3, 383–396.

Voyich, J.M., Vuong, C., DeWald, M., Nygaard, T.K., Kocianova, S., Griffith, S., Jones, J., Iverson, C., Sturdevant, D.E., Braughton, K.R., Whitney, A.R., Otto, M., DeLeo, F.R., 2009. The SaeR/S gene regulatory system is essential for innate immune evasion by Staphylococcus aureus. J. Infect. Dis. 199, 1698–1706.

Winzer, K., Hardie, K.R., Burgess, N., Doherty, N., Kirke, D., Holden, M.T., Linforth, R., Cornell, K.A., Taylor, A.J., Hill, P.J., Williams, P., 2002. LuxS: its role in central metabolism and the in vitro synthesis of 4-hydroxy-5-methyl-3(2H)-furanone. Microbiology 148, 909–922.

Wolz, C., Goerke, C., Landmann, R., Zimmerli, W., Fluckiger, U., 2002. Transcription of clumping factor A in attached and unattached Staphylococcus aureus in vitro and during device-related infection. Infect. Immun. 70, 2758–2762.

Wyatt, M.A., Wang, W., Roux, C.M., Beasley, F.C., Heinrichs, D.E., Dunman, P.M., Magarvey, N.A., 2010. Staphylococcus aureus nonribosomal peptide secondary metabolites regulate virulence. Science 329, 294–296.

Xiong, Y.Q., Van Wamel, W., Nast, C.C., Yeaman, M.R., Cheung, A.L., Bayer, A.S., 2002. Activation and transcriptional interaction between agr RNAII and RNAIII in Staphylococcus aureus in vitro and in an experimental endocarditis model. J. Infect. Dis. 186, 668–677.

Xue, T., Zhao, L., Sun, B., 2013. LuxS/AI-2 system is involved in antibiotic susceptibility and autolysis in Staphylococcus aureus NCTC 8325. Int. J. Antimicrob. Agents 41, 85–89.

Yu, D., Zhao, L., Xue, T., Sun, B., 2012. Staphylococcus aureus autoinducer-2 quorum sensing decreases biofilm formation in an icaR-dependent manner. BMC Microbiol. 12, 288.

Zarkadis, I.K., Mastellos, D., Lambris, J.D., 2001. Phylogenetic aspects of the complement system. Dev. Comp. Immunol. 25, 745–762.

Zhao, L., Xue, T., Shang, F., Sun, H., Sun, B., 2010. Staphylococcus aureus AI-2 quorum sensing associates with the KdpDE two-component system to regulate capsular polysaccharide synthesis and virulence. Infect. Immun. 78, 3506–3515.